Opto-Electronic Advances

Supplementary information

2022, Vol. 5, No. 4

DOI: 10.29026/oea.2022.210014

Cylindrical vector beams reveal radiationless anapole condition in a resonant state

Yudong Lu[1], Yi Xu[2]*, Xu Ouyang[1,2], Mingcong Xian[2], Yaoyu Cao[1], Kai Chen[1] and Xiangping Li[1]*

[1]Guangdong Provincial Key Laboratory of Optical Fiber Sensing and Communications, Institute of Photonics Technology, Jinan University, Guangzhou 510632, China; [2]Department of Electronic Engineering, College of Information Science and Technology, Jinan University, Guangzhou 510632, China.

*Correspondence: Y Xu, E-mail: yi.xu@osamember.org; XP Li, E-mail: xiangpingli@jnu.edu.cn

This file includes:

Supplementary information for this paper is available at https://doi.org/10.29026/oea.2022.210014

Open Access This article is licensed under a Creative Commons Attribution 4.0 International License.
To view a copy of this license, visit http://creativecommons.org/licenses/by/4.0/.

© The Author(s) 2022. Published by Institute of Optics and Electronics, Chinese Academy of Sciences.

Section 1: Numerical methods

The tight focusing of azimuthally polarized (AP) and radially polarized (RP) beams can be evaluated by the vectorial diffraction theory[1,2]. Then the calculated electromagnetic field components associated with the tightly focused AP and RP at an off-focused plane are used as excitation sources for the finite-difference time-domain method to evaluate the optical scattering between the structured light and nanoparticle, where the nanoparticle is located at the focal plane of the AP or RP beam. A nonuniform grid with the smallest grid size of 1 nm as well as the perfectly matched layer boundary conditions are adopted in the numerical simulation.

By using the Cartesian electromagnetic multipole decomposition method[3], we can decompose the contributions of the induced electromagnetic multipole moments to total scattering of the nanoparticle. For convenience, we repeat here the expressions of multipole moments calculated by utilizing the induced currents $\boldsymbol{J}(\boldsymbol{r})$ in the unit cell of the metasurface and the decomposition of radiation power. The induced Cartesian multipole moments can be calculated by:

$$P_\alpha = \frac{1}{\mathrm{i}\omega}\int \mathrm{d}^3 r J_\alpha(\boldsymbol{r}),$$

$$T_\alpha = \frac{1}{10c}\int \mathrm{d}^3 r\left[(\boldsymbol{r}\cdot\boldsymbol{J}(\boldsymbol{r}))r_\alpha - 2r^2 J_\alpha(\boldsymbol{r})\right],$$

$$M_\alpha = \frac{1}{2c}\int d^3 r[\boldsymbol{r}\times\boldsymbol{J}(\boldsymbol{r})]_\alpha,$$

$$Q^{\mathrm{E}}_{\alpha,\beta} = \frac{1}{\mathrm{i}2\omega}\int \mathrm{d}^3 r\left[r_\alpha J_\beta(\boldsymbol{r}) + r_\beta J_\alpha(\boldsymbol{r}) - \frac{2}{3}\delta_{\alpha,\beta}(\boldsymbol{r}\cdot\boldsymbol{J}(\boldsymbol{r}))\right],$$

$$Q^{\mathrm{M}}_{\alpha,\beta} = \frac{1}{3c}\int \mathrm{d}^3 r\left[(\boldsymbol{r}\times\boldsymbol{J}(\boldsymbol{r}))_\alpha r_\beta + (\boldsymbol{r}\times\boldsymbol{J}(\boldsymbol{r}))_\beta r_\alpha\right],$$

$$Q^{\mathrm{T}}_{\alpha,\beta} = \frac{1}{28c}\int d^3 r\left[4r_\alpha r_\beta(\boldsymbol{r}\cdot\boldsymbol{J}(\boldsymbol{r})) - 5r^2(r_\alpha J_\beta + r_\beta J_\alpha) + 2r^2(\boldsymbol{r}\cdot\boldsymbol{J}(\boldsymbol{r}))\delta_{\alpha,\beta}\right],$$

$$O^{\mathrm{E}}_{\alpha,\beta,\gamma} = \frac{1}{\mathrm{i}6\omega}\int \mathrm{d}^3 r\left[J_\alpha(\boldsymbol{r})\left(\frac{r_\beta r_\gamma}{3} - \frac{1}{5}r^2\delta_{\beta,\gamma}\right) + r_\alpha\left(\frac{J_\beta(\boldsymbol{r})r_\gamma}{3} + \frac{r_\beta J_\gamma(\boldsymbol{r})}{3} - \frac{2}{5}(\boldsymbol{r}\cdot\boldsymbol{J}(\boldsymbol{r}))\delta_{\beta,\gamma}\right)\right] + \{\alpha\leftrightarrow\beta,\gamma\} + \{\alpha\leftrightarrow\gamma,\beta\}$$

$$O^{\mathrm{M}}_{\alpha,\beta,\gamma} = \frac{15}{2c}\int \mathrm{d}^3 r\left(r_\alpha r_\beta - \frac{r^2}{5}\delta_{\alpha,\beta}\right)\cdot[\boldsymbol{r}\times\boldsymbol{J}(\boldsymbol{r})]_\gamma + \{\boldsymbol{\alpha}\leftrightarrow\boldsymbol{\beta},\gamma\} + \{\boldsymbol{\alpha}\leftrightarrow\gamma,\boldsymbol{\beta}\}.$$

Here, μ_0 is the permeability of vacuum, ω is the angular frequency, c is the speed of light and $\boldsymbol{r}$ specifies the location where the induced current $\boldsymbol{J}$ is evaluated and $\alpha, \beta = x, y, z$. The radiation power of each multipole can be calculated by:

$$\sigma_P = \frac{\mu_0\omega^4}{12\pi c}|\boldsymbol{P}|^2, \sigma_T = \frac{\boldsymbol{\mu}_0\boldsymbol{\omega}^4\boldsymbol{k}^2}{12\pi c}|\boldsymbol{T}|^2, \tag{S1}$$

$$\sigma_{\mathrm{M}} = \frac{\mu_0\omega^4}{12\pi c}|\boldsymbol{M}|^2, \sigma_{\mathrm{Q^E}} = \frac{\boldsymbol{\mu}_0\boldsymbol{\omega}^4\boldsymbol{k}^2}{40\pi c}\sum_{\boldsymbol{\alpha},\boldsymbol{\beta}}\left|Q^{\mathrm{E}}_{\boldsymbol{\alpha},\boldsymbol{\beta}}\right|^2, \sigma_{\mathrm{Q^M}} = \frac{\boldsymbol{\mu}_0\boldsymbol{\omega}^4\boldsymbol{k}^2}{160\pi c}\sum_{\boldsymbol{\alpha},\boldsymbol{\beta}}\left|Q^{\mathrm{M}}_{\boldsymbol{\alpha},\boldsymbol{\beta}}\right|^2, \tag{S2}$$

Section 2: Fabrication of silicon nanodisks

The Si nanodisk shown in Fig. 5(b) and 5c is fabricated on a glass substrate with a height h = 160 nm and a radius r = 150 nm. First of all, polystyrene spheres (PS) are spin-coated on to a Si film deposited on the glass. The size of the PS is reduced by the RIE process using oxygen gas. And then such PS spheres serve as the mask for the subsequent fluorine-based inductively coupled plasma reactive ion etching (ICP-RIE) using CHF_3 gas. Finally, the PS mask was removed with sonication in acetone. The sizes of the resulting silicon disks can be precisely tuned by changing the size of the PS mask with accurate control of the etching time. The Si nanodisks generated by this method are initially in amorphous phase (a-Si). A femtosecond laser (690–1100 nm, Chameleon, Coherent) with a suitable power level (100 μW) is used to anneal the as prepared Si nanodisk for 10 second. The amorphous Si nanodisk can be transformed into crystalline phase that can improve the scattering properties of the Si nanodisks[4].

Section 3: Dark-field scattering spectroscopy

A home-built spectroscopy setup is used to measure the dark-field scattering of a single Si nanodisk under the excitation of tightly focused AP and RP beams. A femtosecond laser (690–1100 nm, Chameleon, Coherent) with a ultra-low power (3 μW) is shaped by the Fourier spatial filter before it enters liquid crystal polarization converter (ARCoptix) that is used to convert the Gaussian beam to AP and RP beams. Such power level is optimized to ensure no modification of the physical properties of Si nanodisk under excitation. The generated AP and RP beams are shown in Fig. S1. Then, the generated AP and RP beams are focused by a microscope objective lens whose numerical aperture is 1.4. Index matching oil is used to eliminate reflection from the substrate. The sample is mounted on a three-dimensional stage. Then the back scattering signal is collected by the same objective lens and directed by a beam splitter. The dark-field scattering images and back scattering spectra of the sample are recorded by a CCD camera and a spectrometer (Andor).

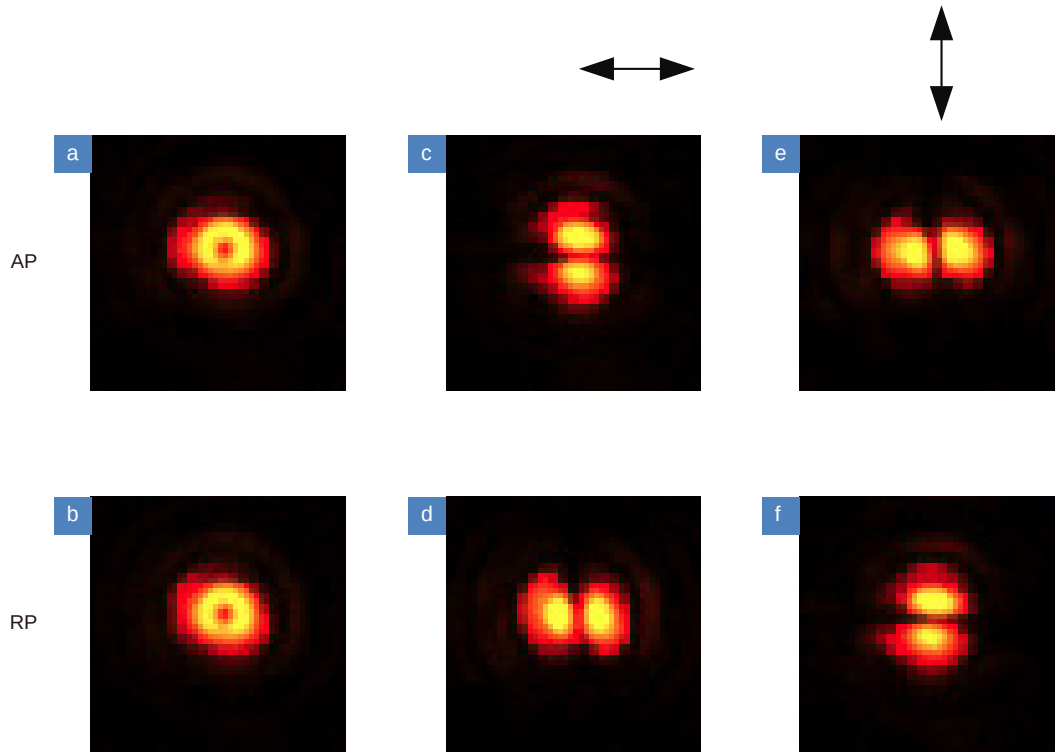

Fig. S1 | Experimentally generated (**a**) AP and (**b**) RP beams and the beam profiles (**c**–**f**) after passing different linear polarizer outlined in the insets. The black arrows indicate the orientations of the polarizer. These beam profiles are focused by a lens (f = 25 cm) and then inspected using a camera.

References

1. Youngworth KS, Brown TG. Focusing of high numerical aperture cylindrical-vector beams. *Opt Express* **7**, 77–87 (2000).
2. Zhan QW, Leger JR. Focus shaping using cylindrical vector beams. *Opt Express* **10**, 324–331 (2002).
3. Radescu EE, Vaman G. Exact calculation of the angular momentum loss, recoil force, and radiation intensity for an arbitrary source in terms of electric, magnetic, and toroid multipoles. *Phys Rev E* **65**, 046609 (2002).
4. Zywietz U, Evlyukhin AB, Reinhardt C, Chichkov BN. Laser printing of silicon nanoparticles with resonant optical electric and magnetic responses. *Nat Commun* **5**, 3402 (2014).